

Hyperfine Structure of the $(6p)^3$ Configuration of Bi^{209}

Donald A. Landman

New York University, Bronx, New York 10453

and

IBM Watson Laboratory, New York, New York 10025

and

Allen Lurio

IBM Watson Laboratory, New York, New York 10025

(Received 24 October 1969)

By means of the atomic-beam-magnetic-resonance method we have measured the $^2P_{3/2}$ level hfs and the $^2P_{3/2}$ and $^2P_{1/2}$ level g_J factors of the Bi^{209} $(6p)^3$ ground configuration. Our experimental results are: $A(^2P_{3/2}) = 491.028(1)$ MHz, $B(^2P_{3/2}) = 978.639(9)$ MHz, $C(^2P_{3/2}) = 0.0193(5)$ MHz, $g_J(^2P_{1/2}) = 0.6654(2)$ and $g_J(^2P_{3/2}) = 1.26083(12)$. In order to interpret these measurements, we have examined the fine structure and the hfs of all the $(6p)^3$ levels. Our calculations show that the inclusion of spin-spin, orbit-orbit, and spin-other-orbit interactions do not improve the theoretical fit to the observed fine structure intervals. The effects of core polarization and relativity can be estimated by writing the dipole hfs Hamiltonian in the form

$$\mathcal{H} = 2\mu\mu_B \vec{I} \cdot \sum_i [\langle r_i^{-3} \rangle_i \vec{I}_i - \sqrt{10} \langle r_i^{-3} \rangle_i (sC^2)_i^{(1)} + \langle r_i^{-3} \rangle_i \vec{s}_i].$$

This analysis of the dipole hfs yields a value $\langle r^{-3} \rangle_{6p}(\text{hfs}) = 1.02 \times 10^{26} \text{ cm}^2$ compared to the fine structure result $\langle r^{-3} \rangle_{6p}(\text{fs}) = 1.25 \times 10^{26} \text{ cm}^2$. With these results we find $Q = -0.383(40)$ b and $\Omega = 0.55(3)\mu_N \text{ b}$.

I. INTRODUCTION

The ground electronic configuration of bismuth is $(6s)^2(6p)^3$ which gives rise to the five levels $^4S_{3/2}$, $^2D_{3/2,5/2}$ and $^2P_{1/2,3/2}$. The ordering of these and nearby levels is shown in Fig. 1. The isolation of these p^3 levels from the levels of other bismuth configurations and the parity-selection rule for electric dipole transitions leads one to expect the 2P and 2D levels to be metastable. Although electric quadrupole and magnetic dipole transitions between the levels have been observed,¹ our measurements show that the lifetime of each of the 2P levels is of the order of a msec or longer. It is probable that the lifetime of each of the 2D levels is even longer.²

The experimental part of our work is the measurement of the g_J values of the $^2P_{1/2}$ and $^2P_{3/2}$ levels and the measurement of the hfs of the $^2P_{3/2}$ level.

In order to properly interpret these measurements we have found it necessary to examine in detail the fine structure (fs) and the hfs of all the $(6p)^3$ levels. This effort has been aided by a number of recent accurate hfs measurements involving

this configuration.³ Our analysis shows that one can obtain a nuclear electric quadrupole moment and a nuclear magnetic octupole moment consistent with all the measurements in the $(6p)^3$ levels.

II. APPARATUS AND EXPERIMENTAL METHOD

The atomic-beam apparatus and detection system have been described previously.^{4,5} In brief, the metastable atoms in the beam were produced by cross-electron bombardment of the ground-state beam and detected by causing the refocused beam to strike a cesium coated surface and de-excite. The electrons produced by the resulting Auger deexcitation of the metastable state were amplified by an electron multiplier and recorded.

The source of the bismuth atoms was a molybdenum oven heated by electron bombardment. In order to minimize the number of bismuth molecules in the beam, the oven was preferentially heated at the top near the slit and intentionally cooled at the bottom by conduction to the oven support. In this way, it was expected that the higher temperature near the slit would produce more

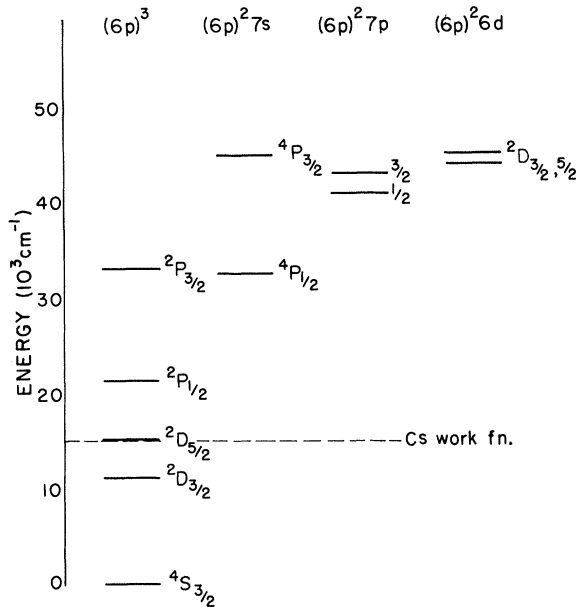


FIG. 1. Energy-level diagram of the low-lying levels in bismuth. The position of the Cs work function is shown to indicate the energy at which our metastable state detector becomes sensitive.

complete dissociation.

III. EXPERIMENTAL RESULTS

Identification of the metastable $^2P_{3/2}$ and $^2P_{1/2}$ beam components was made by comparing the theoretically predicted $\Delta F = 0$, $|\Delta M_F| = 1$ low-field Zeeman transition frequencies with those observed.

A schematic energy-level diagram for the $^2P_{3/2}$ level hfs in an applied magnetic field is given in Fig. 2. The search and measurement procedures for low-field hfs transitions were identical to those previously described.⁵ Some of the results are shown in Table I. After making the small field-dependent corrections (where necessary), we obtain the values for the hfs separations shown in Table II. The error quoted in each of these (and subsequent) results is three times the standard deviation of the mean. We did not measure the $^2P_{1/2}$ level hfs ($\Delta\nu \sim 56\,000$ MHz)⁶ since a high-frequency source was not available. A value for g_I and $g_J(^2P_{1/2})$ can be obtained from an analysis of intermediate-field Zeeman transition data for the $^2P_{1/2}$ level (see the first-half of Table III). We find, after taking account of nonlinear Zeeman terms,

$$g_{F=5} = \frac{1}{10} g_J(^2P_{1/2}) - \frac{9}{10} g_I = 0.06608(3),$$

$$g_{F=4} = -\frac{1}{10} g_J(^2P_{1/2}) - \frac{11}{10} g_I = -0.06710(2),$$

$$\text{giving } g_I = -\frac{1}{2} (g_5 + g_4) = 0.00051(2),$$

$$g_J(^2P_{1/2}) = \frac{1}{2} (11g_5 - 9g_4) = 0.6654(2).$$

In all our work, the magnetic field was calibrated by observing Zeeman transitions in the metastable $(3s3p)^3P_2$ and 3P_1 levels of the even ($I=0$) Mg isotopes; we take $g_J(\text{Mg}) = 1.50114$.⁵ Our result for g_I is somewhat larger than the previously measured more precise value: $g_I = 0.0004887$.⁷ The small deviation of $g_J(^2P_{1/2})$ from its single-configuration theoretical value of 0.6659 (the $J = \frac{1}{2}$ level is independent of coupling in the p^3 configuration) is presumably due to a combination of relativistic,⁸ diamagnetic,⁸ and configuration-mixing effects. Analysis of the intermediate field $\Delta F = 0$, $F = 6$ data for the $^2P_{3/2}$ level (see the second-half of Table III) gives

$$g_{F=6} = \frac{1}{4} g_J(^2P_{3/2}) - \frac{3}{4} g_I = 0.31485(3);$$

and thus (using the more precise g_I value) we get

$$g_J(^2P_{3/2}) = 1.26083(12).$$

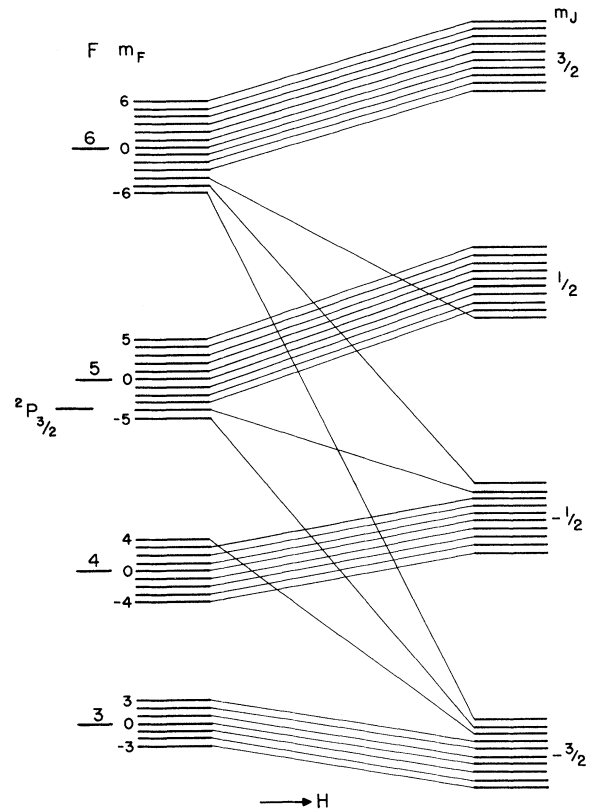


FIG. 2. Schematic diagram of the Zeeman effect of the $(6p)^3\ ^2P_{3/2}$ level of Bi^{209} .

TABLE I. Experimental low-field hfs data: ${}^2P_{3/2}$ level (all units are MHz).

Transition	Frequency	$\mu_B H$
$(F, m) \leftrightarrow (F', m')$		
$(6, 3) \leftrightarrow (5, 4)$	3599.416	4.05
$(6, 0) \leftrightarrow (5, -1)$		
$(6, 2) \leftrightarrow (5, 3)$	3598.903	4.05
$(6, -1) \leftrightarrow (5, -2)$		
$(6, 1) \leftrightarrow (5, 2)$	3598.390	4.06
$(6, -2) \leftrightarrow (5, -3)$		
$(6, 0) \leftrightarrow (5, 1)$	3597.877	4.07
$(6, -3) \leftrightarrow (5, -4)$		
$(5, m) \leftrightarrow (4, m \pm 1)$	2251.034	a
$(5, m) \leftrightarrow (4, m \pm 1)$	2251.039	a
$(5, m) \leftrightarrow (4, m)$	2251.039	a
$(5, m) \leftrightarrow (4, m)$	2251.045	a
$(5, m) \leftrightarrow (4, m)$	2251.038	a
$(5, 0) \leftrightarrow (4, 1)$	2251.234	6.46
$(5, 0) \leftrightarrow (4, -1)$	2250.827	
$(4, m) \leftrightarrow (3, m \pm 1)$	1311.932	a
$(4, m) \leftrightarrow (3, m \pm 1)$	1311.924	a
$(4, m) \leftrightarrow (3, m \pm 1)$	1311.920	a
$(4, m) \leftrightarrow (3, m)$	1311.935	a

^aLines overlapped in very small fields.

The deviation from the single-configuration intermediate-coupling value of 1.2515 (see Sec. IV A) again indicates the presence of interconfiguration, etc., effects.

The transit time of the metastable atoms down the apparatus implies a lower limit of about 1 msec for the lifetimes of the ${}^2P_{3/2}$ and ${}^2P_{1/2}$ levels. This is consistent with Garstang's calculated values of 5.7 and 16 msec, respectively.

IV. DISCUSSION OF RESULTS

A. Wave Functions

The $6p^3$ configuration of Bi in intermediate coupling has been considered by several authors,^{2, 9, 10} in their work only the electrostatic and spin-orbit

TABLE II. Zero-field hfs intervals: ${}^2P_{3/2}$ level.

F	$\Delta\nu [F \leftrightarrow (F-1)]$ (MHz)
6	3598.648(5)
5	2251.038(6)
4	1311.930(11)

TABLE III. Experimental intermediate-field data: ${}^2P_{1/2}$ level (all units are MHz).

$\Delta\nu [(5, m) \leftrightarrow (5, m \pm 1)]$	$\Delta\nu [(4, m) \leftrightarrow (4, m \pm 1)]$	$\Delta\nu$ (Mg)
3.682	3.739	83.658
6.213	6.3065	141.093
6.214	6.309	141.123
11.289	11.466	256.557
11.299	11.476	256.663

Experimental intermediate-field data: ${}^2P_{3/2}$ level (all units are MHz).		
m, m'	$\Delta\nu [(6, m) \leftrightarrow (6, m')]$	$\Delta\nu$ (Mg)
6, 4	64.482	293.365
5, 3	63.851	293.365
5, 4	64.126	293.242
4, 3	63.507	293.242
5, 3	57.390	264.700
4, 2	56.904	264.700
6, 4	53.753	246.440
5, 4	53.529	246.440
4, 3	53.097	246.440
6, 4	53.747	246.422
5, 4	53.531	246.422
5, 3	53.312	246.422
4, 3	53.095	246.422
4, 2	52.877	246.422

interactions were included. Since their calculated energy levels and g factors showed significant differences from the observed values we redid the analysis including the additional spin-other-orbit,¹¹ spin-spin,¹¹ and orbit-orbit¹² interactions in hopes of improving the agreement with experiment.

All the additional terms in the energy matrix are expressible in terms of a single radial integral M_0 . The complete matrix elements are given in Table IV where Racah's choice of phases¹³ has been followed. A least-squares fit to the energy levels treating the radial integrals as adjustable parameters yields the values $F_2 = 989.0 \text{ cm}^{-1}$, $\zeta = 10,093 \text{ cm}^{-1}$, and $M_0 = 2.19 \text{ cm}^{-1}$. The results for F_2 and ζ are essentially the same as those in TAS⁹; M_0 is small and positive as expected. The fit to the observed data is, however, not significantly changed (Table V), implying that configuration mixing is responsible for the discrepancies. The configurations most likely to perturb the $(6s)^2(6p)^3$ are those of the type $nsn's(6p)^3$, where $n \leq 6$, $n' > 6$,

TABLE IV. Nonzero matrix elements for the p^3 configuration in intermediate coupling $\langle p^3 SLJM | H | p^3 S' L' J' M \rangle$.

$(SLJ, S' L' J')$	Electrostatic	Spin-orbit	Spin-other-orbit	Spin-spin	Orbit-orbit	Total
${}^2D_{5/2}, {}^2D_{5/2}$	$3F_0 - 6F_2$	0	$-37M_0$	0	0	$3F_0 - 6F_2 - 37M_0$
${}^4S_{3/2}, {}^4S_{3/2}$	$3F_0 - 15F_2$	0	0	0	$60M_0$	$3F_0 - 15F_2 + 60M_0$
${}^4S_{3/2}, {}^2P_{3/2}$	0	$-\zeta_p$	$15M_0$	0	0	$-\zeta_p + 15M_0$
${}^4S_{3/2}, {}^2D_{3/2}$	0	0	0	$-6\sqrt{5}M_0$	0	$-6\sqrt{5}M_0$
${}^2P_{3/2}, {}^2P_{3/2}$	$3F_0$	0	$-\frac{25}{2}M_0$	0	$40M_0$	$3F_0 + \frac{55}{2}M_0$
${}^2P_{3/2}, {}^2D_{3/2}$	0	$-\frac{1}{2}\sqrt{5}\zeta_p$	$\frac{15}{2}\sqrt{5}M_0$	0	0	$-\frac{1}{2}\sqrt{5}\zeta_p + \frac{15}{2}\sqrt{5}M_0$
${}^2D_{3/2}, {}^2D_{3/2}$	$3F_0 - 6F_2$	0	$\frac{11}{2}M_0$	0	0	$3F_0 - 6F_2 + \frac{11}{2}M_0$
${}^2P_{1/2}, {}^2P_{1/2}$	$3F_0$	0	$25M_0$	0	$40M_0$	$3F_0 + 65M_0$

and $(6s)^2(6p)^2n'p$. Only the first kind, which corresponds to core polarization, will have a large effect on the hfs since unpaired s electrons are involved. Both kinds of configurations may perturb the fine structure, but we have not tried to estimate the size of this perturbation as this seems a formidable task. In Sec. IV B, we will examine further the effect of core polarization on the hfs.

In Table VI, we give the intermediate coupling coefficients for the $J = \frac{3}{2}$ levels in terms of the LS basis and jj basis sets.¹⁴ With the LS basis set, we have

$$|\alpha_{\frac{3}{2}}^{\frac{3}{2}} m\rangle = a_{s\alpha} |{}^4S_{3/2} m\rangle + a_{p\alpha} |{}^2P_{3/2} m\rangle + a_{d\alpha} |{}^2D_{3/2} m\rangle. \quad (1)$$

With the jj basis set, we have

$$|\alpha_{\frac{3}{2}}^{\frac{3}{2}} m\rangle = c_{1\alpha} \left(\frac{3}{2}, \frac{3}{2}, \frac{3}{2}\right)_{3/2}^m + c_{2\alpha} \left(\frac{3}{2}, \frac{3}{2}, \frac{1}{2}\right)_{3/2}^m + c_{3\alpha} \left(\frac{3}{2}, \frac{1}{2}, \frac{1}{2}\right)_{3/2}^m, \quad (2)$$

where (we list only the $m = \frac{3}{2}$ functions)

$$\begin{aligned} \left(\frac{3}{2}, \frac{3}{2}, \frac{3}{2}\right)_{3/2}^{3/2} &= \frac{1}{\sqrt{6}} [p_{3/2}^{3/2} p_{3/2}^{1/2} p_{3/2}^{-1/2}], \\ \left(\frac{3}{2}, \frac{3}{2}, \frac{1}{2}\right)_{3/2}^{3/2} &= \frac{1}{\sqrt{30}} [p_{3/2}^{3/2} p_{3/2}^{-1/2} p_{1/2}^{1/2}] \\ &\quad - \frac{2}{\sqrt{30}} [p_{3/2}^{3/2} p_{3/2}^{1/2} p_{1/2}^{-1/2}], \\ \left(\frac{3}{2}, \frac{1}{2}, \frac{1}{2}\right)_{3/2}^{3/2} &= \frac{1}{\sqrt{6}} [p_{3/2}^{3/2} p_{1/2}^{-1/2} p_{1/2}^{1/2}], \end{aligned} \quad (3)$$

and $[] \equiv$ antisymmetrize. The transformation between the two basis sets is given in Appendix A. We use these wave functions in the following hfs analysis.

B. hfs Interaction Constants

The zero-field hfs intervals for the ${}^2P_{3/2}$ level can be written to second order as

$$\Delta\nu(6 \leftrightarrow 5) = 6A + \frac{2}{3}B + \frac{16}{3}C + h^{-1}(W_6^{(2)} - W_5^{(2)}),$$

$$\Delta\nu(5 \leftrightarrow 4) = 5A - \frac{5}{24}B - \frac{65}{6}C + h^{-1}(W_5^{(2)} - W_4^{(2)}),$$

TABLE V. Intermediate-coupling results for the $(6p)^3$ configuration of Bi.

Level	Energy ^a (cm ⁻¹)	Expt-Calc TAS ^b	Expt-Calc Present work	g_J Expt	g_J LS	g_J TAS ^b	g_J Present work
${}^2D_{5/2}$	15 438	-305	-149	1.20 ^a	1.2005	1.2005	1.2005
${}^4S_{3/2}$	0	377	304	1.6433 ^c (2)	2.0023	1.6379	1.6371
${}^2P_{3/2}$	33 165	184	244	1.2608 ^d (1)	1.3311	1.2519	1.2514
${}^2D_{3/2}$	11 419	-235	-316	1.225 ^e	0.7995	1.2461	1.2473
${}^2P_{1/2}$	21 661	-22	-84	0.6654(2)	0.6659	0.6659	0.6659

^aC. E. Moore, Atomic Energy Levels, Natl. Bur. Standards Circ. 3, 467 (1958).

^bThese columns give the results of a least-squares fit to the energy levels using the values $F_2 = 990$ cm⁻¹, $\zeta_p = 10\,100$ cm⁻¹, and $M_0 = 0$ cm⁻¹ given in TAS Sec. 3¹¹.

^cR. S. Title and K. F. Smith, Phil. Mag. 5, 1281 (1960).

^dPresent work.

^eP. Zeeman, E. Back, and S. Goudsmit, Z. Phys. 66, 1 (1930).

TABLE VI. Intermediate coupling coefficients for the $(6p^3)$ configuration of Bi.

	$^4S_{3/2}$	$^2P_{3/2}$	$^2D_{3/2}$
$a_{s\alpha}$	0.753 39	0.307 06	-0.581 48
$a_{p\alpha}$	0.538 35	-0.795 79	0.277 28
$a_{d\alpha}$	0.377 60	0.521 95	0.764 85
$c_{1\alpha}$	0.173 49	0.982 55	-0.067 07
$c_{2\alpha}$	-0.309 81	0.119 10	0.943 31
$c_{3\alpha}$	-0.934 84	0.142 87	-0.325 07

$$\Delta\nu(4 \rightarrow 3) = 4A - \frac{2}{3}B + \frac{208}{21}C + h^{-1}(W_4^{(2)} - W_3^{(2)}), \quad (4)$$

where A , B , and C are the nuclear magnetic dipole, electric quadrupole, and magnetic octupole hfs interaction constants and

$$W_F^{(2)} = \sum'_{(r,J')} \langle \beta \frac{3}{2} \gamma J F M_F | \mathcal{H}_{\text{hfs}} | \beta \frac{3}{2} \gamma' J' F M_F \rangle^2 \times [W(\gamma J) - W(\gamma' J')]^{-1} \quad (5)$$

is the second-order energy contribution due to other fine-structure levels. $[W(\gamma J) - W(\gamma' J')]$ is the fine-structure separation and the prime on the summation means that $\gamma' J' \neq \gamma J$. β and γ stand for all other nuclear and electronic quantum numbers necessary to specify the state. Neglecting the second-order terms we get the uncorrected values shown in Table VII.

The significant second-order energy contributions come from the other $(6p)^3$ levels. They can be calculated from a knowledge of the $6p$ electron dipole and quadrupole interaction constants in conjunction with the wave functions of Table VI.

Following Sandars and Beck's¹⁵ and Bordarier, Judd, and Klapisch's¹⁶ relativistic treatment of hfs using LS -coupled states, we have

$$\begin{aligned} \mathcal{H}_{\text{hfs}} &= \sum_k T_n^{(k)} \cdot [\sum_i T_e(i)^{(k)}]_{\text{eff}} \\ &= \vec{I} \cdot \sum_i \vec{X}_i + \frac{3}{2} \{ \vec{I} \vec{I} \}^{(2)} \cdot \sum_i Z_i^{(2)} \\ &\quad + T_n^{(3)} \cdot [\sum_i T_e(i)^{(3)}]_{\text{eff}} + \dots \end{aligned} \quad (6)$$

\vec{X}_i and $Z_i^{(2)}$ are given explicitly in terms of valence-electron radial integrals in Refs. 15 and 16; in Appendix B we derive the form of $[T_e^{(k)}(i)]_{\text{eff}}$ for a p electron. The nonzero reduced matrix elements of $\sum_i [T_e^{(k)}(i)]_{\text{eff}}$ for $k=1, 2$, and 3 in the p^3 configuration using the LS basis set are given in Table VIII where the individual electron interaction constants a' , a'' , and a''' are defined by Breit and Wills¹⁰ and $b_{3/2}$ and $c_{3/2}$ are defined by Lurio, Mandel, and Novick.¹⁷ The parameter

TABLE VII. hfs interaction constants and second-order energy corrections for the $^2P_{3/2}$ level (all units are MHz).

	Uncorrected	Corrected
A	491.026(1)	491.028(1)
B	978.569(9)	978.639(9)
C	0.0207(5)	0.0193(5)
	$W_6^{(2)} = 0.049$	
	$W_5^{(2)} = 0.096$	
	$W_4^{(2)} = 0.114$	
	$W_3^{(2)} = 0.056$	

η is given by Schwartz.¹⁸

The constants A , B , and C are given by the following formulas:

$$\begin{aligned} A(\alpha J) &= \frac{1}{IJ} \langle \beta II | I_0 | \beta II \rangle \langle \alpha J J | \sum_i (\vec{X}_i)_0 | \alpha J J \rangle \\ &= \frac{1}{J} \begin{pmatrix} J & 1 & J \\ -J & 0 & J \end{pmatrix} \langle \alpha J | \sum_i \vec{X}_i | \alpha J \rangle, \end{aligned}$$

TABLE VIII. Nonvanishing reduced matrix elements of $\sum_i [T_e^{(k)}(i)]_{\text{eff}}$ for $k=1, 2$, and 3 in the p^3 configuration.

$(SLJ, S' L' J')$	$\langle p^3 SLJ \sum_i X_i p^3 S' L' J' \rangle$
$(^2D_{5/2}, ^2D_{5/2})$	$(\sqrt{\frac{21}{11}})(4a' + a'')$
$(^2D_{5/2}, ^4S_{3/2})$	$-2(\sqrt{\frac{3}{5}})(a' - 2a''' - a'')$
$(^2D_{5/2}, ^2D_{3/2})$	$2(\sqrt{\frac{1}{15}})(2a' + 5a''' - 2a'')$
$(^4S_{3/2}, ^4S_{3/2})$	$\frac{1}{3}(\sqrt{\frac{3}{5}})(10a' + 16a''' - a'')$
$(^4S_{3/2}, ^2D_{3/2})$	$-\frac{2}{3}(\sqrt{\frac{3}{5}})(a' - 2a''' - a'')$
$(^2D_{3/2}, ^2D_{3/2})$	$\frac{1}{3}(\sqrt{\frac{1}{15}})(49a' - 80a''' - 4a'')$
$(^2P_{3/2}, ^2P_{3/2})$	$\sqrt{15} a''$
$(^2P_{3/2}, ^2P_{1/2})$	$2\sqrt{3} a'''$
$(^2P_{1/2}, ^2P_{1/2})$	$(\sqrt{\frac{3}{2}}) a''$
	$\langle p^3 SLJ \sum_i Z_i^{(2)} p^3 S' L' J' \rangle$
$(^2D_{5/2}, ^2P_{3/2})$	$\frac{1}{12}(\sqrt{\frac{7}{3}})\eta b_{3/2}$
$(^2D_{5/2}, ^2P_{1/2})$	$-\frac{1}{8}(\sqrt{\frac{1}{6}})b_{3/2}$
$(^4S_{3/2}, ^2P_{3/2})$	$\frac{1}{54}\sqrt{5}(1-\eta)b_{3/2}$
$(^4S_{3/2}, ^2P_{1/2})$	$-\frac{1}{54}\sqrt{5}(1-\eta)b_{3/2}$
$(^2D_{3/2}, ^2P_{3/2})$	$\frac{1}{108}(5+4\eta)b_{3/2}$
$(^2D_{3/2}, ^2P_{1/2})$	$\frac{1}{108}(4+5\eta)b_{3/2}$
	$\langle p^3 SLJ \sum_i T_e^{(3)}(i) p^3 S' L' J' \rangle$
$(^2D_{5/2}, ^2D_{5/2})$	$\frac{1}{\Omega} 12(\sqrt{\frac{7}{5}})c_{3/2}$
$(^4S_{3/2}, ^2D_{3/2})$	$-\frac{1}{\Omega} 4\sqrt{7}c_{3/2}$
$(^2D_{3/2}, ^2D_{3/2})$	$-\frac{1}{\Omega} 2(\sqrt{\frac{7}{5}})c_{3/2}$
$(^2P_{3/2}, ^2P_{3/2})$	$-\frac{1}{\Omega} 2\sqrt{35}c_{3/2}$

$$\begin{aligned}
B(\alpha J) &= 4\sqrt{\frac{3}{2}} \langle \beta II | \{ \vec{I} \vec{I} \}^{(2)} | \beta II \rangle \\
&\quad \times \langle \alpha JJ | \sum_i (Z_i)^{(2)} | \alpha JJ \rangle \\
&= 2I(2I-1) \begin{pmatrix} J & 2 & J \\ -J & 0 & J \end{pmatrix} \langle \alpha J | \sum_i Z_i^{(2)} | \alpha J \rangle, \quad (7)
\end{aligned}$$

$$\begin{aligned}
C(\alpha J) &= \langle \beta II | (T_n)^{(3)} | \beta II \rangle \\
&\quad \times \langle \alpha JJ | \sum_i [T_e(i)]^{(3)} | \alpha JJ \rangle \\
&= -\Omega \begin{pmatrix} J & 3 & J \\ -J & 0 & J \end{pmatrix} \langle \alpha J | \sum_i T_e(i)^{(3)} | \alpha J \rangle,
\end{aligned}$$

where Ω is the nuclear magnetic octupole moment. From Table VIII and Appendix A, we have

$$\begin{aligned}
A(^2D_{5/2}) &= \frac{4}{5} a' + \frac{1}{5} a'', \\
A(\alpha^{\frac{3}{2}}) &= \frac{1}{45} [(50a_{s\alpha}^2 + 49a_{d\alpha}^2 + 45a_{p\alpha}^2 - 4\sqrt{5}a_{s\alpha}a_{d\alpha}) a' \\
&\quad - (5a_{s\alpha}^2 + 4a_{d\alpha}^2 - 4\sqrt{5}a_{s\alpha}a_{d\alpha}) a'' \\
&\quad + 8(10a_{s\alpha}^2 - 10a_{d\alpha}^2 + \sqrt{5}a_{s\alpha}a_{d\alpha}) a'''] \\
&= (1 + \frac{1}{5} c_{2\alpha}^2) a' - c_{2\alpha}^2 \frac{1}{5} a'' - 4\sqrt{\frac{2}{5}} c_{2\alpha} (c_{1\alpha} - c_{3\alpha}) a''', \\
A(^2P_{1/2}) &= a'', \\
B(^2D_{5/2}) &= 0, \\
B(\alpha^{\frac{3}{2}}) &= \frac{2}{3} a_{p\alpha} [2(1-\eta) a_{s\alpha} + \sqrt{5}(1 + \frac{4}{5}\eta) a_{d\alpha}] b_{3/2} \\
&= [(c_{3\alpha}^2 - c_{1\alpha}^2) - 2\sqrt{\frac{2}{5}} \eta c_{2\alpha} (c_{1\alpha} + c_{3\alpha})] b_{3/2}, \\
B(^2P_{1/2}) &= 0, \\
C(^2D_{5/2}) &= -2c_{3/2}, \\
C(\alpha^{\frac{3}{2}}) &= [a_{p\alpha}^2 + \frac{1}{5} a_{d\alpha} (a_{d\alpha} + 4\sqrt{5} a_{s\alpha})] c_{3/2} \\
&= (c_{1\alpha}^2 - \frac{4}{5} c_{2\alpha}^2 + c_{3\alpha}^2) c_{3/2}, \\
C(^2P_{1/2}) &= 0.
\end{aligned} \quad (8)$$

The dipole constant results agree with the previous work of Breit and Wills¹⁰; the sign difference with the quadrupole constant work of Schuler and Schmidt¹⁹ is explained by our choice of phase for the $^2P_{3/2}$ level wave function which is the negative of theirs.

Several coupling-independent predictions can be made from the results of Eq. (8):

$$\sum_{\alpha=1}^3 A(\alpha, J=\frac{3}{2}) = \frac{16}{5} a' - \frac{1}{5} a'',$$

$$\begin{aligned}
\sum_{\alpha=1}^3 B(\alpha, J=\frac{3}{2}) &= 0, \\
\sum_{\alpha=1}^3 C(\alpha, J=\frac{3}{2}) &= \frac{6}{5} c_{3/2}.
\end{aligned} \quad (9)$$

These equations follow from the fact that the intermediate-coupling coefficients for either basis set of wave functions are the elements of a unitary matrix which transforms the starting basis set of wave functions into the intermediate-coupling wave functions. Hence c_{ij} , (and a_{ij}) satisfy the equations $\sum_i c_{ij} c_{ik} = \sum_i c_{ji} c_{ki} = \delta_{jk}$.

For a pure p^3 configuration, the ratios a''/a' and a'''/a' can be estimated if one knows the relevant relativistic and normalization correction factors.^{18,20} Specifically,

$$\begin{aligned}
\frac{a''}{a'} &= 5\theta = 5 \frac{F_{1/2}}{F_{3/2}} \left| \frac{C''}{C'} \right|^2, \\
\frac{a'''}{a'} &= \frac{5}{16} \frac{C''}{C'} \frac{G}{F_{3/2}}.
\end{aligned} \quad (10)$$

We can estimate C''/C' in two ways: (i) from our experimental value for $\eta = -(C''/C') S/R_{3/2} = 1.55$ (see below), and (ii) by extrapolating Schwartz's calculations¹⁸ of θ for p electron configurations to $Z = 83$ [$\theta(\text{Bi}) = 2.49$]. The results are shown in Table IX; $Z_i = Z - 4$ was used throughout. The ex-

TABLE IX. Parameters and results of core-polarization calculation.

	From $\eta = 1.55$	Schwartz ^a ($\theta = 2.49$)
$-\frac{C''}{C'}$	1.245	1.14
$\frac{a''}{a'}$	14.86	12.5
$\frac{a'''}{a'}$	-0.394	-0.362
a'		
from $\langle v_i^{-3} \rangle$	736 MHz	832 MHz
a'		
from $\langle v_{sC}^{-3} \rangle$	736 MHz	891 MHz
a'_{av}	736 MHz	862 MHz
$\langle v^{-3} \rangle_{\text{core}}$	$-0.91 \times 10^{26} \text{ cm}^{-3}$	$-1.00 \times 10^{26} \text{ cm}^{-3}$
$\langle v^{-3} \rangle_p$	$0.94 \times 10^{26} \text{ cm}^{-3}$	$1.10 \times 10^{26} \text{ cm}^{-3}$

^aReference 17.

perimental dipole hfs for all five of the p^3 levels can be fitted to within several percent by the values $a' = 351$ MHz, $a'' = 11\,310$ MHz, and $a''' = -678$ MHz. These experimentally determined hfs constants yield the ratios $a''/a' = 32.2$ and $a'''/a' = -1.93$, in disagreement with theory. This result is not surprising since an analysis of other heavy element p -electron hfs (viz., Tl) has shown that core polarization of the $s \rightarrow s'$ type has a drastic effect on the hfs. Bleany,²¹ Sandars and Beck,¹⁵ and Woodgate²² have discussed the effect of core polarization and relativity on hfs. They show it is better to parametrize the hfs in terms of three different radial integrals, $\langle r_i^{-3} \rangle$, $\langle r_{sC}^{-3} \rangle$, and $\langle r_s^{-3} \rangle$. In their notation we would write

$$\begin{aligned} \mathfrak{H}C &= 2\mu\mu_B \vec{I} \cdot \sum_i [\langle r_i^{-3} \rangle_i \vec{I}_i \\ &\quad - \sqrt{10} \langle r_{sC}^{-3} \rangle_i (sC^{(2)})_i^{(1)} + \langle r_s^{-3} \rangle_i \vec{S}_i], \end{aligned} \quad (11)$$

where μ is the nuclear dipole moment, μ_B is the Bohr magneton, and i sums over all electrons. A comparison with the previous form of the p^3 hfs dipole Hamiltonian yields the correspondences:

$$\begin{aligned} \langle r_i^{-3} \rangle &= \frac{Ih}{\mu\mu_B} \frac{1}{12} (5a' - 4a''' + a'') \\ &= 2.05 \times 10^{26} \text{ cm}^{-3}, \\ \langle r_{sC}^{-3} \rangle &= \frac{Ih}{\mu\mu_B} \frac{5}{18} (-a' + 2a''' + a'') \\ &= 4.165 \times 10^{26} \text{ cm}^{-3}, \\ \langle r_s^{-3} \rangle &= \frac{Ih}{\mu\mu_B} \frac{1}{18} (10a' + 16a''' - a'') \\ &= -1.62 \times 10^{26} \text{ cm}^{-3}, \end{aligned} \quad (12)$$

where a is in units of Hz and $\mu = 1.08$. In the absence of core polarization and relativity, $\langle r_s^{-3} \rangle$ would be zero. It is interesting to see if we can separate out the $s \rightarrow s'$ core-polarization dependence, since this only contributes to $\langle r_s^{-3} \rangle$ and other types of core polarization have a small effect on the hfs, i. e., for those cases in which this kind of analysis has been done, $\langle r_i^{-3} \rangle = \langle r_{sC}^{-3} \rangle$ to within a percent when relativistic corrections are included. Using the theoretical a ratios in the expressions for $\langle r_i^{-3} \rangle$ and $\langle r_{sC}^{-3} \rangle$ and writing $\langle r_s^{-3} \rangle = Ih/\mu\mu_B \frac{1}{18} (10 + 16a'''/a' - a''/a') a' + \langle r_s^{-3} \rangle_{\text{core}}$, we obtain the values shown in Table IX (to calculate $\langle r_s^{-3} \rangle_{\text{core}}$ in the second column, we used the average $a' = 862$ MHz). The agreement of the two values for a' as derived from η is striking; however, the spread in a' , using Schwartz's values, is still

small ($\sim 7\%$). It is unfortunate that the calculation is so sensitive to the value of C''/C' . Average values of $\langle r^{-3} \rangle$ for the p electrons, $\langle r^{-3} \rangle_p$, can be obtained from the a'_{av} results and are listed in the Table. The fs yields the value $\langle r^{-3} \rangle_p = 1.25 \times 10^{26} \text{ cm}^{-3}$, supporting the larger value of a' .

The experimental quadrupole interaction constants can all be fitted by a single parameter, $b_{3/2} = -801$ MHz with $\eta = 1.55$. This is shown in Table X and is consistent with the assumption of configuration interaction involving only single electron excitations.

The experimental values for the single electron dipole and quadrupole interaction constants can be used to calculate the $W_F^{(2)}(^2P_{3/2})$ and then the corrected values of $A(^2P_{3/2})$, $B(^2P_{3/2})$, and $C(^2P_{3/2})$. These are given in Table VII. The corrected octupole interaction constants for the $^2P_{3/2}$ and $^4S_{3/2}$ levels can be fitted fairly well by $c_{3/2} = 0.0210$ MHz (Table X).

C. Nuclear Moments

Our result for the magnetic dipole moment uncorrected for the diamagnetic shielding effect $\mu = 4.21(14)$ is $\sim 4\%$ larger than the nuclear resonance value $\mu = 4.03771 \mu_N$. The corrected values are $4.25(14)$ and $4.07970 \mu_N$, respectively.

A value for the electric quadrupole moment can be obtained from the expression

$$Q = \frac{5}{2} \frac{b_{3/2}}{e^2 \langle r^{-3} \rangle_p R(Z_i)}. \quad (13)$$

Taking $b_{3/2} = -801$ MHz, $\langle r^{-3} \rangle_p = 1.135 \times 10^{26} \text{ cm}^{-3}$ (obtained by averaging the fs value with the hfs value), and $Z_i = 79$, we get $Q = -0.385(40)$ b for the nuclear moment without the Sternheimer correction. The quoted uncertainty is derived solely from the uncertainty in $\langle r^{-3} \rangle_p$. This value is in good agreement with a recent optical measurement²³ which gives $Q = -0.379(15)$ b.

We can deduce a value for the magnetic octupole moment from the following relations:

$$\Omega = 7 \frac{c_{3/2}}{a'} \frac{\mu}{I} \frac{a_0^2}{Z^2} \frac{F}{T}, \quad (14a)$$

$$\Omega = \frac{21}{8} \frac{c_{3/2}}{b_{3/2}} \frac{e^2 Q}{\mu_B} \frac{a_0^2}{Z^2} \frac{R}{T}, \quad (14b)$$

$$\Omega = \frac{105}{8} \frac{c_{3/2}}{c_{3/2}^p} \mu_B \frac{a_0^2}{Z^2} \frac{HZ_i}{T}, \quad (14c)$$

TABLE X. Experimental and calculated hfs interaction constants for the $(6p)^3$ configuration of Bi (all units are MHz).

Level	A		B		Exp	C_{corr} Calc
	Exp	Calc	Exp	Calc		
$^2D_{5/2}$	2502 ^a	2550	300(100) ^a	0	b	-0.0419
$^4S_{3/2}$	-446.937(1) ^c	-439	-305.067(2) ^c	-305	0.0183(1) ^c	0.0173
$^2P_{3/2}$	491.026(1) ^d	504	978.639(9) ^d	967	0.0193(5) ^d	0.0204
$^2D_{3/2}$	-1230 ^{a,e}	-1166	-657 ^{a,e}	-662	b	-0.0126
$^2P_{1/2}$	11310 ^a	11310

^aS. Mrozowski, Phys. Rev. **62**, 526 (1942); **69**, 169 (1946).

^bNo measurements.

^cR. J. Hull and G. O. Brink, Ref. 3. These are their corrected values; the uncorrected results are $A = -446.942(1)$ MHz, $B = -304.654(2)$ MHz, and $C = 0.0165(1)$ MHz.

^dPresent work. These are the corrected values.

^eH. Schüler and T. Schmidt, Z. Physik **99**, 717 (1936); E. U. Mintz, J. Franklin Inst. **222**, 613 (1936); F. M. Kelly and L. O. Dickie, Bull. Am. Phys. Soc. **11**, 456 (1966).

where all interaction constants are in Hz, and ζ_p is in cm^{-1} . In (14c), c is the velocity of light. Extrapolating Schwartz's results gives $F/T = 0.850$, $R/T = (R/F)F/T = 0.977$, and $HZ_i/T = (HZ_i/F)F/T = 82.6$. Taking $\mu = 4.08 \mu_N$, we get the following values for Ω : from (14a) $0.63 \mu_N$ b (for $a' = 736$ MHz) and $0.53 \mu_N$ b (for $a' = 862$ MHz); from (14b), $0.52 \mu_N$ b; and from (14c), $0.56 \mu_N$ b. These results are impressively consistent. Averaging the values from the different methods gives $\Omega = 0.55(3) \times \mu_N$ b.

The Bi^{209} nucleus has one $6h_{9/2}$ proton outside of closed proton and neutron shells. Thus one would expect the single-particle model to be fairly reliable. Assuming the nuclear multipole moments arise from the $6h_{9/2}$ proton alone, then gives $\mu = \frac{9}{22}(12g_l - g_s) \mu_N = 2.62 \mu_N$, $Q = -\frac{8}{11}\langle r^2 \rangle_N = -0.221$ b, and $\Omega = \frac{42}{143}(7g_l - g_s)\langle r^2 \rangle_N \mu_N = 0.126 \mu_N$ b, where we have used $g_l = 1.000$, $g_s = 5.586$, and $\langle r^2 \rangle_N = 0.304$ b from electron scattering data.²⁴ These values are seen to be somewhat smaller than, but of the same order of magnitude as, the experimentally derived values.

It is known that if one chooses $g_s = 2$ in the single-particle model calculation of μ , then one obtains very nearly the experimental value. If we use $g_s = 2$ in the single-particle model calculation of Ω we obtain $\Omega = 0.45 \mu_N$ b in much better agreement with experiment. Perhaps there is some significance to this observation.

APPENDIX A

We will write the LS -coupled wave functions for the p^3 configuration using the phases given by Racah. This requires that the sign of all 2P wave functions given in matrix table $(6m)^{25}$ of TAS, and the signs of all elements of the p^3 spin-orbit interaction table²⁵ of TAS be multiplied by -1 . We

also choose the sign of the square root in the expression for $R(k3)$ given by Inglis and Johnson such that each intermediate-coupling wave function goes over to the pure LS -coupled wave function (as $\zeta \rightarrow 0$) with a $+1$ phase factor. This requires we use a minus sign for the $k=1$ square root in $R(k3)$. The typographical errors in Inglis and Johnson²⁶ are corrected in the paper by Lindgren and Johansson,⁹ but note, that for our choice of phases, $R(k2) = -(\epsilon_k + 3x)R(k3)$. Finally, we note that in pure jj coupling the state which connects to $\psi(^4S_{3/2})$ has the coefficient $c_3 = -1$. With the above conditions we find

$$c_{1\alpha} = \frac{1}{3\sqrt{2}}(2a_{s\alpha} - 3a_{p\alpha} + \sqrt{5}a_{d\alpha}),$$

$$c_{2\alpha} = -\frac{1}{3}(\sqrt{5}a_{s\alpha} - 2a_{d\alpha}),$$

$$c_{3\alpha} = -\frac{1}{3\sqrt{2}}(2a_{s\alpha} + 3a_{p\alpha} + \sqrt{5}a_{d\alpha});$$

$$\text{and } a_{s\alpha} = \sqrt{\frac{2}{3}}(c_{1\alpha} - \sqrt{\frac{5}{2}}c_{2\alpha} - c_{3\alpha}),$$

$$a_{p\alpha} = -\frac{1}{\sqrt{2}}(c_{1\alpha} + c_{3\alpha}),$$

$$a_{d\alpha} = \frac{1}{3}\sqrt{\frac{5}{2}}(c_{1\alpha} + 2\sqrt{\frac{2}{5}}c_{2\alpha} - c_{3\alpha}).$$

The parameter α takes the values 1, 2, and 3 since there are three $J = \frac{3}{2}$ states.

APPENDIX B

According to Sandars and Beck,¹⁵ we have

$$[T_e(i)^{(k)}]_{\text{eff}} = \sum_{k_s, k_l} P_i^{(k_s, k_l)k} U_i^{(k_s, k_l)k}, \quad (\text{B1})$$

where $U_i^{(k_s, k_l)k}$ is a Hermitian unit tensor operator of rank k_s in spin space, k_l in orbital space, and

k in the combined spin-orbital space; and

$$P_i^{(k_s, k_l)k} = \frac{(2k_s + 1)(2k_l + 1)}{(2k + 1)^{1/2}} \sum_{j, j'} [(2j + 1)(2j' + 1)]^{1/2} \left\{ \begin{array}{ccc} \frac{1}{2} & \frac{1}{2} & k_s \\ l & l & k_l \\ j & j' & k \end{array} \right\} \langle nlj^R || T_e^{(k)}(i) || nlj'^R \rangle. \quad (\text{B2})$$

The R superscript denotes relativistic states. The reduced matrix elements are given in Refs. 17 and 18.

We consider the case $k = 3$ for a p electron. Because of the triangle condition on the coupling of angular momenta and the fact that only terms with $k_s + k_l + k$ even contribute, the sum in Eq. (B1) reduces to just one term: $P_i^{(1, 2)^3} U_i^{(1, 2)^3}$. From Eq. (B2),

$$P_i^{(1, 2)^3} = 60\sqrt{\frac{1}{7}} \left\{ \begin{array}{ccc} \frac{1}{2} & \frac{1}{2} & 1 \\ 1 & 1 & 2 \\ \frac{3}{2} & \frac{3}{2} & 3 \end{array} \right\} \times \langle P_{3/2}^R || T_e^{(3)} || P_{3/2}^R \rangle = -\frac{1}{\Omega} 10\sqrt{3} c_{3/2}.$$

Finally, using

$$\begin{aligned} & \langle p^3 SLJ || \sum_{i=1}^3 U_i^{(1, 2)^3} || p^3 S'L'J \rangle \\ &= (2J + 1)\sqrt{7} \left\{ \begin{array}{ccc} S & S' & 1 \\ L & L' & 2 \\ J & J & 3 \end{array} \right\} \\ & \times \langle p^3 SL || \sum_{i=1}^3 U_i^{12} || p^3 S'L' \rangle \\ &= (2J + 1)\sqrt{\frac{14}{3}} \left\{ \begin{array}{ccc} S & S' & 1 \\ L & L' & 2 \\ J & J & 3 \end{array} \right\} \langle p^3 SL || V^{12} || p^3 S'L' \rangle, \end{aligned}$$

where $\langle p^3 SL || V^{12} || p^3 S'L' \rangle$ is given in Ref. 12, we obtain the results shown in Table VIII.

¹S. Mrozowski, Phys. Rev. **69**, 169 (1946); M. Hulst and S. Mrozowski, J. Opt. Soc. Am. **54**, 855 (1964); J. Heldt, *ibid.* **58**, 1516 (1968).

²R. H. Garstang, Res. Nat. Bur. Standards **68A**, 61 (1964).

³S. Mrozowski, Phys. Rev. **62**, 526 (1942); L. O. Dickie and F. M. Kelly, Can. J. Phys. **45**, 2249 (1967); P. C. Magnante and H. H. Stroke, J. Opt. Soc. Am. **59**, 836 (1969); R. J. Hull and G. O. Brink, Phys. Rev. A **1**, 685 (1970); R. S. Title and K. F. Smith, Phil. Mag. **5**, 1281 (1960).

⁴A. G. Blachman, D. A. Landman, and A. Lurio, Phys. Rev. **181**, 70 (1969); A. Lurio, *ibid.* **126**, 1768 (1962).

⁵A. G. Blachman, D. A. Landman, and A. Lurio, Phys. Rev. **150**, 59 (1966).

⁶S. Mrozowski, Phys. Rev. **62**, 169 (1946).

⁷Nuclear Data Tables (Academic Press Inc., New York, 1969), Vol. 5, Nos. 5 and 6.

⁸A. Abragam and J. H. Van Vleck, Phys. Rev. **92**, 1448 (1953).

⁹E. U. Condon and G. H. Shortley, *The Theory of Atomic Spectra* (Cambridge University Press, New York, 1935); R. S. Title and K. F. Smith, Phil. Mag. **5**, 1281 (1960), referred to as TAS; I. Lindgren and C. M. Johansson, Arkiv. Fysik **15**, 445 (1959).

¹⁰G. Breit and L. A. Wills, Phys. Rev. **44**, 470 (1933).

¹¹H. H. Marvin, Phys. Rev. **71**, 102 (1947); H. Horie, Progr. Theoret. Phys. (Kyoto) **10**, 296 (1953); T. Yamanouchi and H. Horie, J. Phys. Soc. Japan **7**, 52 (1952); F. R. Innes, Phys. Rev. **91**, 31 (1953).

¹²S. Yanagawa, J. Phys. Soc. Japan **10**, 1029 (1955);

B. G. Wybourne, J. Chem. Phys. **40**, 1457 (1963).

¹³G. Racah, Phys. Rev. **63**, 367 (1943).

¹⁴M. F. Crawford and L. A. Wills, Phys. Rev. **48**, 69 (1935).

¹⁵P. G. H. Sandars and J. Beck, Proc. Roy. Soc. (London) **289**, 97 (1965).

¹⁶Y. Bordarier, B. R. Judd, and M. Klapisch, Proc. Roy. Soc. (London) **289**, 81 (1965).

¹⁷A. Lurio, M. Mandel, and R. Novick, Phys. Rev. **126**, 1758 (1962).

¹⁸C. Schwartz, Phys. Rev. **105**, 173 (1957); **97**, 380 (1955).

¹⁹H. Schüller and T. Schmidt, Z. Physik **99**, 717 (1936).

²⁰H. Kopfermann, *Nuclear Moments* (Academic Press Inc., New York, 1958).

²¹B. Bleaney, in *Proceedings of the International Colloquium No. 164 on Magnetic Hyperfine Structure of Atoms and Molecules, Paris, 1966* (Centre National de la Recherche Scientifique, Paris, 1967), p. 13.

²²G. K. Woodgate, Proc. Roy. Soc. (London) **293**, 117 (1966).

²³G. Eisele, I. Koniordos, G. Müller, and R. Winkler, Phys. Letters **28B**, 256 (1968).

²⁴G. J. C. Van Niftrik and R. Engfer, Phys. Letters **22**, 490 (1966).

²⁵TAS (Ref. 9, pp. 225 and 268).

²⁶D. R. Inglis and M. H. Johnson, Phys. Rev. **38**, 1642 (1931).